

Berry Phase Effect on Exciton Transport and Bose Einstein Condensate

Wang Yao* and Qian Niu

Department of Physics, The University of Texas, Austin, Texas 78712

(Dated: April 23, 2019)

With exciton lifetime much extended in semiconductor quantum-well structures, their transport and Bose-Einstein condensation become a focus of research in recent years. We reveal a momentum-space gauge field in the exciton center-of-mass dynamics due to Berry phase effects. We predict spin-dependent topological transport of the excitons analogous to the anomalous Hall and Nernst effects for electrons. We also predict spin-dependent circulation of a trapped exciton gas and instability in an exciton condensate in favor of vortex formation.

PACS numbers: 71.35.-y, 03.65.Vf, 73.43.-f, 03.75.Kk

In semiconductor, an electron can be excited from the valance band into the conduction band by absorbing a photon. Exciton is a bound state of the extra electron in the conduction band and the hole leaving behind in the valance band. Exciton plays a crucial role in semiconductor optics, as a source of nonlinear optical effects in particular [1]. In a bulk semiconductor, exciton life time is quite short because of recombination annihilation of the electron and hole accompanied by emission of a photon. By confining electrons and holes separately in two coupled quantum wells [2, 3], the resulting indirect exciton can have a life time greatly extended (up to 10 μ s so far [4]), opening up an entirely new realm of exciton physics. It is of great interest to study transport of a metastable exciton gas, which may bring in new functionality of optoelectronics [5, 6]. Moreover, recent experiments suggest that realization of the Bose-Einstein condensation of excitons may finally become in reach after decades of prediction [7, 8, 9, 10].

In this Letter, we study the center of mass dynamics of excitons, finding a momentum-space gauge field due to Berry phase in the basis Bloch functions of the quantum wells as well as in the wavefunction describing the relative motion of the electron and hole pair [11]. The gauge field can lead to spin-dependent exciton transport much like the anomalous Hall and Nernst effects for electrons [12, 13, 14, 15, 16, 17]. As the spin of an exciton is correlated with the polarization of the emitted photon from exciton annihilation, these anomalous transport phenomena may be directly observed from a spatial map of polarization resolved exciton luminescence. The gauge field can also induce circulation in a trapped gas of excitons and a spontaneous vortex formation in an exciton Bose-Einstein condensate.

Gauge structure in exciton wavefunction.—In a homogeneous system, the exciton energy-momentum eigenstate is parameterized by the center-of-mass wavevector \mathbf{q} and the quantum number n for each hydrogen-like orbit of the relative motion. The wavefunction can be generally written as $\Psi_{n,\mathbf{q}}^{\text{ex}} = e^{i\mathbf{q}\cdot\mathbf{R}}U_{n,\mathbf{q}}^{\text{ex}}$ with \mathbf{R} being the center-of-mass coordinate. Like the Bloch function, the exciton wavefunction is decomposed into a plane-wave envelope

function for center-of-mass motion and an ‘internal’ structure $U_{n,\mathbf{q}}^{\text{ex}} = \sum_{\mathbf{k}} F_n(\mathbf{k}, \mathbf{q}) e^{i\mathbf{k}\cdot\mathbf{r}} u_{e,\mathbf{k}+\frac{m_e}{M}\mathbf{q}} u_{h,-\mathbf{k}+\frac{m_h}{M}\mathbf{q}}$ where \mathbf{k} and \mathbf{r} are respectively the wavevector and coordinate for the relative motion. u_{e,\mathbf{k}_e} and u_{h,\mathbf{k}_h} are the periodic part of the electron and hole Bloch function, and $\sum_{\mathbf{k}} F_n(\mathbf{k}, \mathbf{q}) e^{i\mathbf{k}\cdot\mathbf{r}}$ gives the envelope function of the relative motion which may depend on \mathbf{q} in general. $M \equiv m_e + m_h$ is the exciton mass. Similar to that of the Bloch electrons [13], the gauge structure of exciton lies in the dependence of the ‘internal’ structure $U_{n,\mathbf{q}}^{\text{ex}}$ on the dynamical parameter \mathbf{q} [11]. The gauge potential is defined as $\mathcal{A}_\mu^{\text{ex}} \equiv i \langle U^{\text{ex}} | \partial_{q_\mu} | U^{\text{ex}} \rangle$, and the gauge field is then $\Omega^{\text{ex}} \equiv \nabla_{\mathbf{q}} \times \mathcal{A}^{\text{ex}}$. This gauge field, known as the Berry curvature, is analogous to a ‘magnetic’ field in the crystal momentum space. Its integral over a q -space area yields the Berry phase of an exciton state adiabatically going around along the boundary of the area, which is similar to the relationship between a magnetic field and the Arharonov-Bohm phase.

For 2D exciton, the Berry curvature is always normal to the plane with magnitude given by,

$$\begin{aligned} \Omega^{\text{ex}}(\mathbf{q}) = & \left(\frac{m_h}{M}\right)^2 \sum_{\mathbf{k}} |F|^2 \Omega^h\left(-\mathbf{k} + \frac{m_h}{M}\mathbf{q}\right) \\ & + i \sum_{\mathbf{k}} (\partial_{q_x} F^* \partial_{q_y} F - \partial_{q_y} F^* \partial_{q_x} F) \\ & + \frac{m_h}{M} \sum_{\mathbf{k}} \left[\partial_{q_x} |F|^2 \mathcal{A}_y^h\left(-\mathbf{k} + \frac{m_h}{M}\mathbf{q}\right) - x \leftrightarrow y \right] \end{aligned} \quad (1)$$

where $\mathcal{A}_\mu^h(\mathbf{k}) \equiv i \langle u_{h,\mathbf{k}} | \partial_{k_\mu} | u_{h,\mathbf{k}} \rangle$ and $\Omega^h(\mathbf{k}) \equiv \nabla_{\mathbf{k}} \times \mathcal{A}^h(\mathbf{k})$ are respectively the gauge potential and gauge field in the hole band. The Berry curvature of the exciton thus has three parts. On the right hand side of Eq. (1), the **first** term is the inheritance of Berry curvatures from the parent Bloch bands [18]. In quantum well, heavy-light hole mixing at finite in-plane wavevector leads to pronounced Berry curvature distributions in these subbands [16], and we expect this to be the dominant contribution to the exciton Berry curvature [Fig. (1)]. This contribution is *spin dependent* as Ω^h changes sign when hole spin flips. The **second** term is due to the entanglement of relative motion in n th orbit with the center-

of-mass motion. This contribution is spin independent in general, but can have opposite value at \mathbf{q} and $-\mathbf{q}$, analogous to the valley dependent Berry curvature in graphene [19]. It must vanish when the system has both time reversal symmetry and 180° rotation symmetry in the 2D plane [19]. The **third** one is the cross terms of the first two. Its spin dependence comes from the gauge potential \mathcal{A}_μ^h .

Semiclassical Equation of Motion.—From now on, we focus on spatially indirect excitons with long radiative lifetime. To see the effect of Berry curvature, we first establish the semiclassical theory for wavepacket dynamics of excitons subject to perturbations varying slowly in space and time. Consider the following exciton wavepacket centered at center-of-mass coordinate \mathbf{R}_c : $|X\rangle = \int [d\mathbf{q}] w(\mathbf{q}) |\Psi_{\mathbf{q}}^{\text{ex}}\rangle$. $w(\mathbf{q})$ is a function localized around \mathbf{q}_c with a width much smaller than the inverse of the in-plane exciton Bohr radius a_B , and $\int [d\mathbf{q}]$ stands for $\int d\mathbf{q} (2\pi)^{-2}$ here and hereafter. The equation of motion for this wavepacket can be derived from the effective Lagrangian [13],

$$\dot{\mathbf{R}}_c = \frac{\partial \mathcal{E}(\mathbf{q}_c, \mathbf{R}_c)}{\hbar \partial \mathbf{q}_c} - \dot{\mathbf{q}}_c \times \boldsymbol{\Omega}^{\text{ex}}, \quad (2a)$$

$$\hbar \dot{\mathbf{q}}_c = -\frac{\partial \mathcal{E}(\mathbf{q}_c, \mathbf{R}_c)}{\partial \mathbf{R}_c} - \dot{\mathbf{R}}_c \times \mathcal{D}. \quad (2b)$$

$\mathcal{E}(\mathbf{q}_c, \mathbf{R}_c)$ is the semiclassical energy of the exciton wavepacket with center-of-mass wavevector \mathbf{q}_c and coordinate \mathbf{R}_c . To leading order, it is of a factorized form $\mathcal{E}(\mathbf{q}_c, \mathbf{R}_c) \equiv \mathcal{E}_0(\mathbf{q}_c) + V(\mathbf{R}_c)$ where $\mathcal{E}_0(\mathbf{q}_c)$ is the unperturbed exciton dispersion in the homogeneous quantum well and V is the potential energy from spatial dependent external perturbations. Hence, the exciton center-of-mass motion is subjected to a mechanical force $\mathcal{C} \equiv -\nabla V$. In an electrostatic potential ϕ , $\mathcal{C}_{x,y} \equiv ed\partial_{x,y} \frac{\partial \phi}{\partial z}$ with d being the separation between the electron and hole layers [20]. Thus, the intrinsic dipole moment of indirect exciton allows its transport to be controlled by the electric field gradient, which forms the basis of electrically gated excitonic circuits [5, 6]. The dipole moment also allows a *real-space* ‘magnetic’ field $\mathcal{D} \equiv ed \frac{\partial \mathbf{B}_z}{\partial z} \hat{z}$ from the gradient of the external magnetic field $\mathbf{B}(\mathbf{r})$. In conjugation, the Berry curvature $\boldsymbol{\Omega}^{\text{ex}}$ indeed plays the role of a *momentum-space* ‘magnetic’ field which give rises to an anomalous contribution to the velocity [13, 14, 15]. For $1s$ heavy-hole excitons being investigated for transport and condensation phenomena [4, 7, 8, 9, 10], the Berry curvature distribution is opposite between the two ‘bright’ exciton branches $e_+^\dagger h_-^\dagger |G\rangle$ and $e_-^\dagger h_+^\dagger |G\rangle$, and between the two ‘dark’ exciton branches $e_+^\dagger h_+^\dagger |G\rangle$ and $e_-^\dagger h_-^\dagger |G\rangle$ [21]. The exciton center-of-mass motion thus acquires a spin-dependent ingredient.

It is interesting to make a comparison with the spin dependent center-of-mass dynamics recently observed on exciton-polaritons [22], which results from the momen-

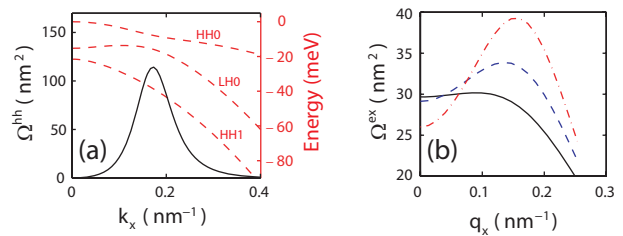


FIG. 1: Gauge structure in a 10nm quantum well. (a) Dashed curves denote the three highest valence subbands. Berry curvature (solid curve) in heavy-hole subband HH0 is most pronounced where HH0 anti-cross with the light-hole subband LHO. In the calculation, we assume a valence barrier height of 140 meV and the same Luttinger parameters ($\gamma_1 = 6.85$, $\gamma_2 = 2.1$, and $\gamma_3 = 2.9$) for the quantum well layer and the barrier. (b) Berry curvature as a function of center-of-mass wavevector for $1s$ heavy-hole exciton. We assume the in-plane exciton Bohr radius $a_B = 8, 10$, and 12 nm for solid, dashed and dash-dotted curves respectively.

tum dependent polarization splitting for spatially direct excitons. Such mechanism is unimportant for indirect excitons where polarization splitting is negligible as the wavefunction overlap between the electron and hole component is small [23]. In addition to the heavy-light hole mixing mechanism discussed here, spin dependent center-of-mass motion of indirect exciton can also arise from Rashba spin-orbit coupling in the parent Bloch bands as first discussed by Wang and Li [24].

Spin Hall effect and Spin Nernst effect.—The above semiclassical equation of motion is the basis for calculation of exciton transport currents driven by mechanical and statistical forces. The exciton current density can be defined as $\mathbf{J} \equiv \int [d\mathbf{q}_c] f \dot{\mathbf{R}}_c$ where $f = f(\mathbf{q}_c, \mathbf{R}_c)$ is the distribution function. In an electrically controlled excitonic circuit [5, 6], the flow of excitons is driven by the ‘electric-like’ force \mathcal{C} from patterned electrodes [20]. We immediately find that the anomalous velocity term in Eq. (2a) contributes a spin-dependent exciton Hall current: $\mathbf{J} = \mathcal{C} \times \frac{1}{\hbar} \int [d\mathbf{q}_c] f(\mathbf{q}_c) \boldsymbol{\Omega}^{\text{ex}}(\mathbf{q}_c)$ [15]. Note that the above Hall current comes mainly from the equilibrium part of carrier distribution and hence is referred as the *intrinsic* contribution, as opposed to the *extrinsic* contribution from the non-equilibrium part of distribution by phonon scattering or disorder scattering [12, 25]. Intrinsic contribution dominates the anomalous Hall effect when phonon scattering is the major cause for exciton momentum relaxation [25].

In most current experiments, hot indirect exciton gas are generated at laser excitation spot, and the exciton temperature decreases by phonon emissions upon diffusion to remote trap regions [7, 8, 9, 10]. ‘Thermoelectric’ responses to the statistical forces of temperature gradient and chemical potential gradient is thus of direct relevance. From the basis of the Einstein relation, it is suggested that an exciton spin Hall current can

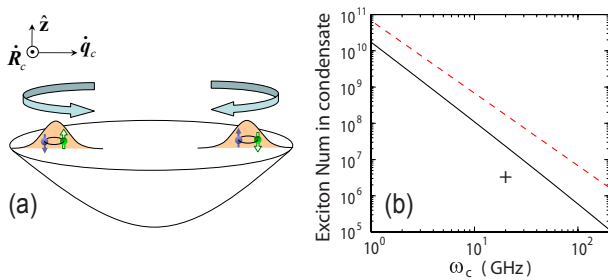


FIG. 2: (a) Motion of indirect excitons in trap. The Berry curvature induces a spin-dependent anomalous velocity transverse to the force from the trap. (b) Critical condensate size as a function of harmonic trap frequency ω_c . Solid curve shows N_{vor} above which the condensate is unstable against vortex formation. Dashed curve denotes N_c for BEC-BCS crossover. For reference, ‘+’ denotes a condensate loaded in a 20 GHz trap [20] with a typical density $3 \times 10^{10} \text{cm}^{-2}$ [7, 9]. We have assumed GaAs coupled quantum well where electron and hole layers are separated by $d = 10$ nm, and the exciton Berry curvature is taken from the $a_B = 10$ nm curve in Fig. 1(b).

be induced by a chemical potential gradient. Furthermore, the Mott relation for the ‘electrical’ conductivity and ‘thermoelectric’ conductivity suggests the *spin Nernst effect*, i.e. spin Hall current driven by a temperature gradient. Both relations are proved to hold for Berry phase supported topological transport currents of Bloch electrons [17], and the conclusion is straightforwardly generalized to excitons of Boson statistics. Specifically, we find the spin-dependent exciton Hall current in the presence of chemical potential gradient and temperature gradient: $\mathbf{J} = -\nabla\mu \times \frac{1}{\hbar} \int [d\mathbf{q}_c] f \Omega^{\text{ex}} - \frac{\nabla T}{T} \times \frac{1}{\hbar} \int [d\mathbf{q}_c] \Omega^{\text{ex}} [(\mathcal{E} - \mu)f - k_B T \log(1 - e^{-\beta(\mathcal{E} - \mu)})]$.

One can extract the Hall conductivity σ and the Nernst conductivity α defined by $J_x = \sigma(C_y - \nabla_y \mu) + \alpha(-k_B \nabla_y T)$. Note that the Berry curvature originated from heavy-light hole mixing is most pronounced in a momentum space region centered around $\mathbf{q} = \mathbf{0}$ (see Fig.1(b)). Therefore, we may approximate $\Omega^{\text{ex}} \propto \theta(\mathcal{E}_s - \mathcal{E})$ where typically $\mathcal{E}_s \sim \text{meV}$. Assuming $k_B T \gg \mathcal{E}_s$, we find

$$\sigma = \frac{1}{\hbar} \frac{\Phi}{2\pi} \frac{\zeta}{1 - \zeta}, \quad \alpha = \frac{1}{\hbar} \frac{\Phi}{2\pi} \frac{\zeta \ln \zeta + (1 - \zeta) \ln(1 - \zeta)}{\zeta - 1}.$$

$\zeta \equiv \exp(\mu/k_B T)$ is the *fugacity* of the exciton gas and $\Phi \equiv \int d\mathbf{q} \Omega^{\text{ex}}(\mathbf{q})$ is the total flux of the Berry curvature. For the typical GaAs quantum wells, we find $\Phi \sim \pi$.

Berry Phase Effect on Exciton Condensate.—In 2D, Bose-Einstein condensation is possible only in a trap [26]. In a confining potential $V(\mathbf{R})$, the anomalous velocity from the Berry curvature results in a spin-dependent circulation motion for uncondensed excitons [Fig. 2(a)]. To consider the Berry phase effect on condensed excitons in trap, we first establish the effective quantum Hamiltonian in presence of the Berry curvature. From Eq. (2), it is evident that, with finite Ω^{ex} , the physical position and

momentum of the exciton wavepacket no longer form a canonical pair. Quantization of the non-canonical form of motion is possible by finding the canonical position and momentum variables \mathbf{R} and \mathbf{q} which are related to the physical ones by: $\mathbf{R}_c = \mathbf{R} + \mathcal{A}(\mathbf{q}); \mathbf{q}_c = \mathbf{q}$ [27]. This is simply a generalization of the Peierls substitution to the momentum-space gauge field. The semiclassical energy of the exciton can then be expressed in terms of the canonical position and momentum variable as $\mathcal{E}(\mathbf{R}, \mathbf{q}) = \mathcal{E}_0(\mathbf{q}) + V(\mathbf{R}) + \nabla V \cdot \mathcal{A}(\mathbf{q})$. Taking the standard quantization procedure, we obtain the modified Gross-Pitaevskii equation with the Berry phase effect

$$\left[-\frac{\nabla^2}{2M} + V + U_0 |\Psi(\mathbf{R})|^2 + \nabla V \cdot \hat{\mathcal{A}} \right] \Psi(\mathbf{R}) = \mu \Psi(\mathbf{R}), \quad (3)$$

where $\hat{\mathcal{A}} \equiv \mathcal{A}(-i\nabla)$ is an operator acting on the condensate wavefunction $\Psi(\mathbf{R})$. $U_0 = e^2 d/\epsilon$ is the strength of the repulsive dipole-dipole interaction between indirect excitons [28]. The last term on the right hand side shows the Berry phase effect. In a harmonic trap $V(\mathbf{R}) = \frac{1}{2} M \omega_c^2 R^2$ with characteristic length $a_{\text{osc}} \equiv (M \omega_c)^{-1/2} \gg a_B$, this term reduces to $\nabla V \cdot \hat{\mathcal{A}} = M \omega_c^2 \Omega_0 \hat{L}_z$ where $\Omega_0 \equiv \Omega^{\text{ex}}(\mathbf{q} = 0)$ and \hat{L}_z is the angular momentum operator.

In the multi-component exciton condensate, the Berry phase term is diagonal in the spin subspace while interconversion between different spin components is incoherent via the exciton spin relaxation processes [29]. We first analyze how the Berry curvature affect each component individually. Obviously, the Berry phase term will lead to a spin-dependent energy correction to the states with finite angular momentum. To create a vortex with a single quantized circulation, the cost of energy in absence of Berry curvature is: $\varepsilon_v = \pi n_0 M^{-1} \ln(0.888 \frac{\rho}{\xi_0})$ [30], where n_0 and ξ_0 are respectively the exciton density and healing length at the trap center without vortex, and ρ is the spatial dimension of the exciton condensation which, in the Thomas-Fermi approximation, is given by $\rho = a_{\text{osc}} (U_0 N M)^{1/4}$. The Berry phase term contribute an energy correction $\Delta \varepsilon_v = M \omega_c^2 \Omega_0 \mathcal{L}_v$ where $\mathcal{L}_v = \pm \frac{1}{2} n_0 \pi \rho^2$ is the angular momentum of the vortex state [30]. When Ω_0 and \mathcal{L}_v have opposite sign, the Berry curvature reduces the energy cost of creating a vortex in the corresponding spin component of the condensate. Further, when $\varepsilon_v + \Delta \varepsilon_v < 0$, a nonrotating condensate component becomes unstable upon forming a vortex. As \mathcal{L}_v is quadratic while ε_v is logarithmic in the condensate size ρ , such instability occurs when the number of condensed excitons is larger than $N_{\text{vor}} \sim (U_0 M^3 \omega_c^2 \Omega_0^2)^{-1}$.

With the increase of density, the excitonic condensate will cross from BEC of tightly bound excitons to BCS type momentum-space e - h pairing [23, 31]. In the harmonic trap, the border size for such crossover is roughly $N_c \sim (U_0^{-1} M \omega_c^2 a_B^4)^{-1}$, corresponding to the density $\sim a_B^{-2}$. Thus, for sufficiently large $U_0 M$, $N_{\text{vor}} \ll N_c$

and the instability is reached well in the BEC end where the above treatment of condensate is valid. In typical GaAs coupled quantum well systems, our calculations show that spontaneous vortex formation in BEC phase is expected in tight confinement which may be realized in electrostatic traps [20] (see Fig. 2(b)).

Conclusions and Outlooks.—We have discussed a gauge structure that naturally exists in exciton wavefunction and the resultant Berry phase effect on exciton dynamics. A direct consequence is the spin-dependent topological transport of excitons driven by mechanical and statistical force, which may add novel spin functionalities into excitonic circuits [5, 6]. Of particular interest is the coupling of the Berry curvature to the angular momentum of a trapped wavefunction which may lead to instability of nonrotating Bose-Einstein condensate above the critical size N_{vor} . The tendency of forming vortex and anti-vortex depends on the spin species. As instability can be simultaneously reached in each spin component under equilibrium, an interesting problem of vortex formation dynamics is posed for future study. If the wavefunctions of different spin components are driven into different angular momentum states, exciton spin relaxation processes can lead to fast depletion of the condensate. Such dynamics may be experimentally probed from the angular distribution of photoluminescence [28].

Bose-Einstein condensation has also been claimed for exciton-polariton systems recently [32]. It will be interesting to investigate the Berry phase effect on polariton condensate since polariton can inherit the Berry curvature from its exciton portion. Because of the lighter mass of polariton, N_{vor} extrapolated from the above analysis suggests that Berry phase effect becomes important only at a much higher density. However, in such case, a dilute BEC may not be the proper description for the polariton condensate [23]. Further studies are needed to have a clear understanding of the Berry phase effects on other phases of the condensate [31, 33].

The work was supported by NSF, DOE, the Welch Foundation, and NSFC.

* wangyao@physics.utexas.edu

- [1] D. S. Chemla and J. Shah, *Nature* **411**, 549 (2001).
- [2] A. Alexandrou *et al.*, *Phys. Rev. B* **42**, 9225 (1990).
- [3] L. V. Butov, A. Zrenner, G. Abstreiter, G. Böhm, and G. Weimann, *Phys. Rev. Lett.* **73**, 304 (1994).
- [4] Z. Voros, R. Balili, D. W. Snoke, L. Pfeiffer, and K. West, *Phys. Rev. Lett.* **94**, 226401 (2005).
- [5] D. W. Snoke, *Photonics Spectra* **40**, 108 (2006).
- [6] A. A. High, A. T. Hammack, L. V. Butov, M. Hanson, and A. C. Gossard, *Opt. Lett.* **32**, 2466 (2007).
- [7] L. Butov, C. W. Lai, A. L. Ivanov, A. C. Gossard, and D. S. Chemla, *Nature* **417**, 47 (2002); L. Butov, A. C. Gossard, and D. S. Chemla, *Nature* **418**, 751 (2002).
- [8] D. Snoke, S. Denev, Y. Liu, L. Pfeiffer, and K. West, *Nature* **418**, 754 (2002); Z. Voros, D. W. Snoke, L. Pfeiffer, and K. West, *Phys. Rev. Lett.* **97**, 016803 (2006).
- [9] S. Yang, A. T. Hammack, M. M. Fogler, L. V. Butov, and A. C. Gossard, *Phys. Rev. Lett.* **97**, 187402 (2006).
- [10] S. Yang, A. V. Mintsev, A. T. Hammack, L. V. Butov, and A. C. Gossard, *Phys. Rev. B* **75**, 033311 (2007).
- [11] M. V. Berry, *Proc. R. Soc. London Ser. A* **392**, 45 (1984).
- [12] S. Murakami, N. Nagaosa, and S.-C. Zhang, *Science* **301**, 1348 (2003); J. Sinova *et al.*, *Phys. Rev. Lett.* **92**, 126603 (2004).
- [13] M.-C. Chang and Q. Niu, *Phys. Rev. B* **53**, 7010 (1996).
- [14] D. J. Thouless, M. Kohmoto, M. P. Nightingale, and M. den Nijs, *Phys. Rev. Lett.* **49**, 405 (1982).
- [15] With Berry curvature explicitly accounted as a band property, the semiclassical approach finds Hall conductance as an integral of Berry curvature over occupied states [13], exactly reproducing the linear response result [14]. The integral of Berry curvature over the Brillion zone as the quantized Hall conductance was first recognized in [14].
- [16] W. Yao, A. H. MacDonald, and Q. Niu, *Phys. Rev. Lett.* **99**, 047401 (2007).
- [17] D. Xiao, Y. Yao, Z. Fang, and Q. Niu, *Phys. Rev. Lett.* **97**, 026603 (2006).
- [18] Conduction band Berry curvature plays a less important role due to the prefactor $\frac{m_e}{M} \ll 1$ when the hole effective mass is much heavier.
- [19] D. Xiao, W. Yao, and Q. Niu, *Phys. Rev. Lett.* **99**, 236809 (2007); W. Yao, D. Xiao, and Q. Niu, arXiv:0705.4683.
- [20] A. T. Hammack *et al.*, *J. Appl. Phys.* **99**, 066104 (2006).
- [21] e_{\pm}^{\dagger} denotes the creation operator for electron in the conduction subband with $S_z = \pm\frac{1}{2}$, and h_{\pm}^{\dagger} for hole in the heavy-hole subband HH0 arising from the $J_z = \mp\frac{3}{2}$ band-edge state.
- [22] A. Kavokin, G. Malpuech, and M. Glazov, *Phys. Rev. Lett.* **95**, 136601 (2005); C. Leyder *et al.*, *Nature Physics* **3**, 628 (2007); W. Langbein *et al.*, *Phys. Rev. B* **75**, 075323 (2007).
- [23] P. B. Littlewood *et al.*, *J. Phys.: Condens. Matter* **16**, S3597 (2004).
- [24] J. W. Wang and S. S. Li, *Appl. Phys. Lett.* **91**, 052104 (2007).
- [25] C. Zeng, Y. Yao, Q. Niu, and H. H. Weitering, *Phys. Rev. Lett.* **96**, 037204 (2006).
- [26] V. Bagnato and D. Kleppner, *Phys. Rev. A* **44**, 7439 (1991).
- [27] C. P. Chu, M. C. Chang, and Q. Niu, arXiv:0709.1407 (2007).
- [28] J. Keeling, L. S. Levitov, and P. B. Littlewood, *Phys. Rev. Lett.* **92**, 176402 (2004).
- [29] M. Z. Maialle, E. A. de Andrada e Silva, and L. J. Sham, *Phys. Rev. B* **47**, 15776 (1993).
- [30] C. J. Pethick and H. Smith, *Bose-Einstein Condensation in Dilute Gases* (Cambridge University Press, Cambridge, 2002), 1st ed.
- [31] T. Hakioglu and M. Sahin, *Phys. Rev. Lett.* **98**, 166405 (2007).
- [32] J. Kasprzak *et al.*, *Nature* **443**, 409 (2006); H. Deng, G. S. Solomon, R. Hey, K. H. Ploog, and Y. Yamamoto, *Phys. Rev. Lett.* **99**, 126403 (2007); R. Balili, V. Hartwell, D. Snoke, L. Pfeiffer, and K. West, *Science* **316**, 1007 (2007).
- [33] J. W. Ye, arXiv:0712.0437 (2007).